Gene Therapy (2013) **20,** 24 – 34

www.nature.com/gt

ORIGINAL ARTICLE

Engineered human Tmpk fused with truncated cell-surface markers: versatile cell-fate control safety cassettes

M Scaife[1], N Pacienza[2], BCY Au[2], JCM Wang[2,3], S Devine[1], E Scheid[4], C-J Lee[2], O Lopez-Perez[2], A Neschadim[1], DH Fowler[5], R Foley[4] and JA Medin[1,2,3]

Cell-fate control gene therapy (CFCGT)-based strategies can augment existing gene therapy and cell transplantation approaches by providing a safety element in the event of deleterious outcomes. Previously, we described a novel enzyme/prodrug combination for CFCGT. Here, we present results employing novel lentiviral constructs harboring sequences for truncated surface molecules (CD19 or low-affinity nerve growth factor receptor) directly fused to that CFCGT cDNA (TmpkF105Y). This confers an enforced one-to-one correlation between cell marking and eradication functions. *In-vitro* analysis demonstrated the full functionality of the fusion product. Next, low-dose 3′-azido-3′-deoxythymidine (AZT) administration to non-obese diabetic/severe combined immunodeficiency (NOD/SCID) mice injected with transduced clonal K562 cells suppressed tumor growth; furthermore, one integrated vector on average was sufficient to mediate cytotoxicity. Further, in a murine xenogeneic leukemia-lymphoma model we also demonstrated *in-vivo* control over transduced Raji cells. Finally, in a proof-of-principle study to examine the utility of this cassette in combination with a therapeutic cDNA, we integrated this novel CFCGT fusion construct into a lentivector designed for treatment of Fabry disease. Transduction with this vector restored enzyme activity in Fabry cells and retained AZT sensitivity. In addition, human Fabry patient $CD34^+$ cells showed high transduction efficiencies and retained normal colony-generating capacity when compared with the non-transduced controls. These collective results demonstrated that this novel and broadly applicable fusion system may enhance general safety in gene- and cell-based therapies.

Gene Therapy (2013) **20,** 24–34; doi:10.1038/gt.2011.210; published online 12 January 2012

Keywords: lentivirus; cell-fate control; TMPK; AZT

INTRODUCTION

Transplantation of hematopoietic stem cells and lymphocytes is a curative treatment for inherited and acquired disorders. However, complications can limit the safety of allogenic and autologous transplantation. One complication is graft-versus-host disease. Likewise, recent serious adverse events regarding the use of genetically modified T cells expressing synthetic chimeric antigen receptors for generating antitumor immunity have also highlighted the need for safer protocols.[1,2]

Cell-fate control gene therapy (CFCGT)-based strategies can be used universally where any cell is transduced with therapeutic vectors or transplanted outside of its normal context. To date, the most widely used CFCGT system is the herpes simplex virus thymidine kinase gene (HSV-TK) that confers ganciclovir (GCV) sensitivity to transduced cells. Phase I–II clinical trials have shown safety and proof-of-principle outcomes with the HSV-TK/GCV system; however, they have also uncovered a number of areas where improvements can be made.[3,4] First, limited persistence of HSV-TK gene-modified cells due to the immunogenicity of the foreign transgene product has been reported.[5] Second, HSV-TK escape variants have been identified that evade prodrug-mediated deletion.[6–8] Third, the kinetics of GCV activation are suboptimal and overexpression of HSV-TK mostly shifts the rate-limiting step in GCV activation to the next enzyme in the pathway, guanylate kinase.[9] In light of the above limitations, efforts have been made to improve the existing HSV-TK/GCV system, such as by identifying variants with improved enzyme kinetics, or combining it with guanylate kinase overexpression.[10–12] Recently, another CFCGT system has been implemented in the clinic.[13,14] There a chemical agent (AP1903) facilitates the activation of a human-modified caspase-9 by mediating dimerization and inducing apoptosis of the engineered T cells. Even though the initial results show the abrogation of early graft-versus-host disease events due to a rapid eradication of modified T cells; however, this CFCGT system requires more study concerning the use of such a dimerizer and long-term clinical implementation.

To overcome major shortcomings of existing cell-fate control systems, we previously described human thymidylate kinase (Tmpk) mutant enzymes combined with the prodrug 3′-azido-3′-deoxythymidine (AZT) as a novel CFCGT system.[15] A single amino-acid substitution resulted in a minimally modified mutant Tmpk enzyme (TmpkF105Y) with increased catalytic activity for AZT.[16,17] As described by Sato *et al.*,[15] overexpression of the TmpkF105Y variant mediated by a recombinant lentiviral vector (LV) renders cells extremely sensitive to normally non-toxic AZT, leading to apoptosis via two mechanisms: phosphorylated AZT can be incorporated into DNA during cell replication causing termination of elongated chains, and activated AZT can lead to the loss of mitochondrial membrane potentials and increased cleavage of caspase-3 leading to apoptosis independent of cell-cycle status.

Our previously described cell-fate control gene delivery platform consisted of a bicistronic LV containing the cDNAs of the

[1]Department of Medical Biophysics, University of Toronto, Toronto, Ontario, Canada; [2]Ontario Cancer Institute, University Health Network, Toronto, Ontario, Canada; [3]Institute of Medical Sciences, University of Toronto, Toronto, Ontario, Canada; [4]Department of Pathology and Molecular Medicine, Centre for Gene Therapeutics, McMaster University, Hamilton, Ontario, Canada and [5]Experimental Transplantation and Immunology Branch, National Cancer Institute, National Institutes of Health, Bethesda, MD, USA. Correspondence: Professor JA Medin, University Health Network, Canadian Blood Services Building, 67 College Street, Room 406, Toronto, Ontario, Canada M5G 2M1. E-mail: jmedin@uhnres.utoronto.ca
Received 28 March 2011; revised 1 December 2011; accepted 2 December 2011; published online 12 January 2012

mutant Tmpk and truncated human CD19 (CD19Δ) as a cell-surface marker separated by an internal ribosome entry site (IRES).[15] However, that system was hampered somewhat by disjointed expression due to the IRES element between the mutant Tmpk effector enzyme and the cell-surface molecule, which can be used to enrich, track and even eliminate vector-positive cells.[18] Inclusion of that basal IRES element in the vector backbone also diminished applicability concerning tandem addition of other therapeutic cDNAs.

To obviate the above issue, we have generated novel LV constructs that engineer the expression of directly in-frame fused, truncated cell-surface markers with TmpkF105Y. The first iteration is a truncated human CD19 fused to the mutant Tmpk (LV/CD19ΔTmpkF105Y), and the second is a fully human, codon-optimized (CO), truncated low-affinity nerve growth factor receptor (LNGFR) fused to the mutant Tmpk (LV/LNGFRΔTmpkF105Y). Thus, both LVs confer an enforced one-to-one correlation between the cell marking and eradication functions. We hypothesized that creating such fusion enzymes would still allow Tmpk dimerization, maybe even facilitate it, while this tethering to the cell membrane via the cell-surface marker component may enhance activation of AZT by localizing the enzyme at the cellular entry site of the prodrug.

In the present study, we demonstrated that AZT-mediated cell killing enabled by these novel fusion enzymes is at least as effective as was previously observed for mutant Tmpk alone. *In-vitro* studies and *in-vivo* analyses involving two independent models confirmed the broad applicability of these constructs. Further, to demonstrate the contextual utility of this fusion cassette, we also generated a therapeutic LV for the correction of Fabry disease. Fabry disease is a lysosomal storage disorder due to a deficiency in the activity of α-galactosidase A (α-gal A). Indeed, we have previously demonstrated that Fabry disease can be corrected systemically by LV-mediated gene therapy targeting hematopoietic stem cells.[19] However, even with these encouraging results, there are still concerns of insertional mutagenesis with integrating vectors leading to leukemogenesis as exemplified from past X-linked severe combined immunodeficiency (SCID) clinical trials.[20,21] As such, we demonstrate here vigorous α-gal A expression and AZT-mediated cell killing. Thus, these fusion enzyme systems may serve as robust identification and safety cassettes to supplement existing cell- and gene-based therapies.

RESULTS

Synthesis of novel LVs engineering expression of mutant Tmpk fused to cell-surface molecules

Figure 1 shows schemas of the recombinant LVs we have constructed for these studies. The first LV, CD19ΔTmpk, was constructed by fusing the truncated human CD19 cDNA in-frame to the N-terminal residue of human mutant Tmpk (TmpkF105Y). A second cell-fate control fusion cassette was also generated using the cell-surface marker LNGFRΔ that has already been used in clinical trials.[3] To further enhance the expression of the second construct, the entire human LNGFRΔTmpk cassette was fully CO before synthesis; ~22% of the sequence was ultimately replaced by optimal codons (data not shown).

To assess fusion protein expression levels engineered by the novel cell-fate control LVs, K562 cells were infected a single time at a functional multiplicity of infection (MOI) of 10. Under these conditions, the transduced K562 cells were found to be ~15% CD19, or ~20% LNGFR positive, respectively (data not shown). Transduced cell pools were expanded in culture and enriched for transgene expression by fluorescent-activated cell sorting (FACS). Cells were found to stably express truncated human CD19 or LNGFR, with enriched populations >98% positive compared with the non-transduced (NT) controls (Figure 2a). A western blot for Tmpk expression was next performed on lysates from the transduced K562 cells (Figure 2b). All samples, including controls, demonstrated a background band at ~24 kDa, which is the expected size for wild-type Tmpk. The K562 cell line over-expressing the mutant Tmpk (non-fusion) was derived previously in our laboratory.[15] These cells showed a marked overexpression of Tmpk compared with the NT controls. As expected, cells expressing the CD19ΔTmpk or LNGFRΔTmpk fusion proteins showed a band of increased molecular weight (~60kDa) confirming that Tmpk is fused to its truncated cell-surface molecules and is stably expressed.

Characterization of clonally-derived populations of transduced K562 cells

A robust cell-fate control system should be able to mediate induced killing with relatively low transgene expression levels and with only one integrated vector copy number. Therefore by limiting-dilution cloning of the enriched, transduced K562 cell populations, we established eight cell lines that demonstrated stable expression of variable amounts of truncated human CD19 (Figure 3a) to perform functional quantification studies. On the

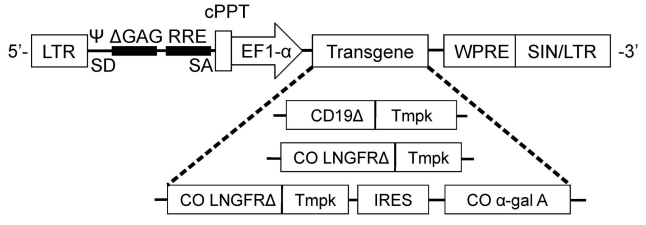

Figure 1. Schemas of the novel recombinant lentiviral vectors constructed for these studies. CD19ΔTmpk, truncated human CD19 fused to mutant human thymidylate kinase (TmpkF105Y); LNGFRΔTmpk, truncated CO human LNGFR molecule fused to TmpkF105Y; cPPT, central polypurine tract; EF1-α, elongation factor 1-α promoter; LTR, long terminal repeat; RRE, Rev responsive element; SA, 3 splice acceptor site; SD, 5 splice donor site; SIN, self-inactivating LTR; ψ, human immunodeficiency virus packaging signal.

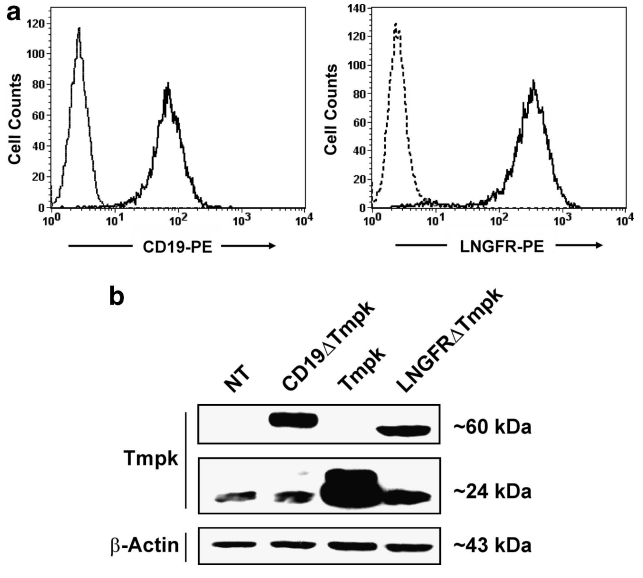

Figure 2. Expression of mutant human Tmpk fused to cell-surface molecules following LV transduction of K562 cells. (**a**) Flow cytometry analysis for truncated CD19 or LNGFR expression. (**b**) Western blot demonstrating Tmpk fusion expression compared with mutant Tmpk overexpression alone.

a

Clone	MFI	ABC
NT	18.6	10,515
L1	220.7	76,098
L2	**106.5**	**24,873**
L3	131.0	31,609
L5	226.7	80,736
H2	316.2	194,028
H5	**361.9**	**303,482**
H10	406.8	471,069
H12	582.9	2,644,748

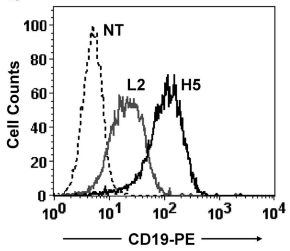

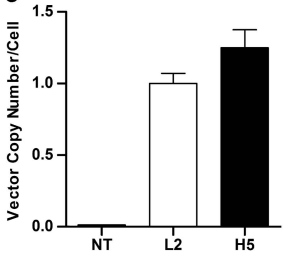

Figure 3. Characterization of LV/CD19ΔTmpk transduced K562 clonal populations. (**a**) Flow cytometry quantification of various K562 single cell-derived clones demonstrating differential expression levels of CD19ΔTmpk based on CD19 ABC assays. (**b**) Representative CD19 staining histogram with low (L2) and high (H5) expressing clones. (**c**) Real-time PCR results on K562 genomic DNA showing vector copy number. Data are mean ± s.e.m. ($n = 3$). NT, non-transduced negative control.

protein level, clone H5 ($CD19^{High}$) showed a 12-fold increase in CD19 antibody binding capacity (ABC) compared with clone L2 ($CD19^{Low}$) (303 482 versus 24 873 ABC) (Figure 3a). These differences in the CD19 ABC of clones H5 and L2 are recapitulated in the representative flow cytometry histograms (Figure 3b). Importantly, there were no observed differences in cell proliferation or viability among the different clones, even when supranormal levels of the fusion transgene were being expressed (data not shown). Quantitative real-time PCR of genomic DNA prepared from the transduced cells showed that both clones H5 and L2 contained ~1 copy of the integrated provirus per cell (Figure 3c).

Sensitivity of clonally derived transduced K562 cells to AZT

Next, we tested the sensitivity of the characterized K562 transduced cell clones to the prodrug, AZT. We incubated low and high CD19 expressing K562 clones with increasing concentrations of AZT for 3 days and examined the incidence of apoptosis on day 4 by Annexin V staining. As shown in Figure 4a, both clones undergo apoptosis in a dose-dependent manner when treated with increasing concentrations of AZT. As expected, K562 clones expressing higher levels of mutant Tmpk demonstrated more Annexin V staining, likely due to increased phosphorylation of AZT to its toxic metabolites. At AZT concentrations of 10 μM, clone H5 showed nearly an eightfold increase in the apoptotic index, compared with a fourfold increase for clone L2. In addition, cell viability was measured independently by the MTS assay after exposure to increasing concentrations of AZT (Figure 4b). The high-expressing clone appeared to be more sensitive to AZT, but of particular interest, the lower expressing clone was ultimately still eradicated to a similar extent, demonstrating the robust sensitivity of this system. Further, both clones selectively demonstrated significant cytotoxicity at concentrations as low as 0.1 μM AZT ($P < 0.001$ compared with NT control). Indeed, transduced cells were minimally viable after exposure to any AZT, and at higher concentrations of the prodrug (>1 μM), no cells could be expanded in the longer term (data not shown).

In-vivo killing of low- and high-expressing clonally derived K562 CD19ΔTmpk-transduced cells in a subcutaneous tumor model

We next examined killing of the low- and high-expressing CD19ΔTmpk-transduced K562 clones in an *in-vivo* tumor model. In all, 1×10^7 transduced or control cells were injected subcutaneously into the dorsal flanks of non-obese diabetic/severe combined immunodeficiency (NOD/SCID) mice. To minimize variation between animal groups, low- and high-expressing K562 clones (L2 and H5) were injected into the left and right flanks, respectively, of the same animal. Starting 1 day after cell inoculation, the mice received daily injections of AZT at concentrations of 17.1 mg kg^{-1} per day for a period of 2 weeks. This drug concentration was calculated based on the FDA recommended dose of 1200 mg per day (17.1 mg kg^{-1} per day for an average 70 kg individual) for acute treatment of HIV infection in humans.[15,22] Mice were killed when control tumors reached the maximal allowable size of ~1500 mm^3, which occurred ~24 days after cell injection. As shown in Figure 5a, mice that received the NT K562 cells and AZT treatment quickly developed large tumors in a time-dependent manner. Likewise, mice that received the L2 and H5 CD19ΔTmpk clones without AZT treatment also developed large tumors in the same time-dependent manner. In contrast, growth of the low- and high-fusion protein expressing tumors in animals receiving AZT was strongly inhibited. At the point of kill, tumors from all mice (if any were present) were extracted and weighed. As shown in Figure 5b, there were striking differences in tumor masses between the AZT-treated and non-treated mice. Both clones showed significant reduction in tumor mass ($P < 0.005$), with no statistical differences ($P = 0.197$) between them. This emphasizes that minimal transgene expression may also be sufficient to mediate Tmpk/AZT killing *in vivo*. As well, there was no statistical difference between the tumor masses of NT K562 cells in animals that received AZT, compared with the tumors not treated with AZT (low and high, $P = 0.288$, $P = 0.844$, respectively). This shows that there is only specific cytotoxicity against transduced K562 cells and not against parental cells at these clinically-relevant doses of AZT.

Although cell killing was quite robust with AZT, some mice of the experimental group did grow tumors, although of a significantly smaller size than those in the control group. A major concern highlighted from HSV-TK/GCV clinical trials was that some cells evaded drug sensitivity due to the spontaneous mutations in the transgene and loss of effector enzyme expression.[6] Accordingly, we investigated the possibility that some K562 clonal cells had escaped drug sensitivity. To evaluate this, we extracted and examined these tumor cells more extensively *in vitro*. After the tumors were weighed at the time of euthanasia, they were mechanically and enzymatically processed to allow for expansion of remaining (if any) cells *in vitro*. Within a few weeks of expansion, these cells were assayed for CD19 expression by flow cytometry and for sensitivity to AZT. As shown in Figures 5c and d, all cells that were expanded remained CD19 positive and were still sensitive to AZT in a dose-dependent manner ($P < 0.001$) at concentrations as low as 1 μM.

Enhanced survival with AZT addition of NOD/SCID mice harboring LV/LNGFRΔTmpk-transduced human leukemic cells

We next asked whether LV/LNGFRΔTmpk transduction could enhance survival of AZT-treated NOD/SCID mice in a murine xenogeneic tumor model of lymphoid leukemia. For this, Raji cells (human Burkitt's lymphoma B-cell line) were transduced and enriched by FACS (Figure 6a). *In-vitro* cytotoxicity assays showed

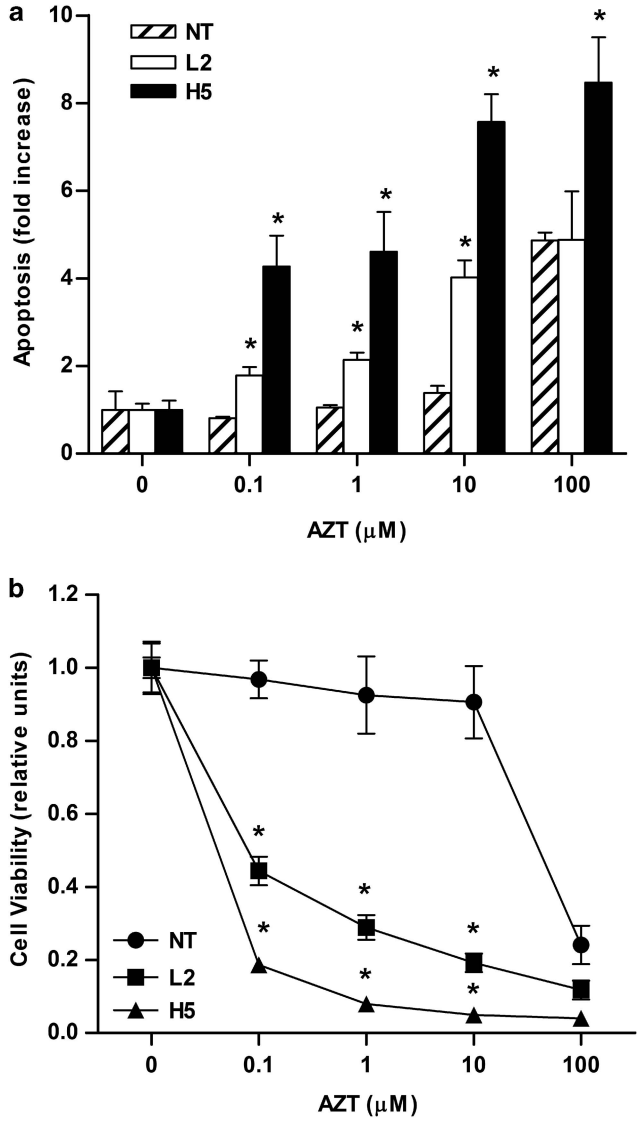

Figure 4. Sensitivity of the clonally derived K562 cells transduced with LV/CD19ΔTmpk to 3′-azido-3′-deoxythymidine (AZT). (**a**) Annexin V/propidium iodide staining of cells after 3 days of treatment of AZT. Data are mean ± s.e.m. ($n = 2$). Data are normalized to non-treated controls. The statistical significance between groups was calculated by the two-tailed, Student's *t*-test, $^*P < 0.001$ compared with the NT control. (**b**) Cell viability was measured by proliferation MTS assay following 4 days of AZT treatment. Data are mean ± s.e.m. ($n = 4$). Data are normalized to non-treated controls. The statistical significance between groups was calculated by the two-tailed, Student's *t*-test, $^*P < 0.001$ compared with the NT control.

that the pool of transduced Raji cells were selectively sensitive to AZT in a drug dose-dependent manner with significant viability loss at concentrations as low as 0.1 μM AZT ($P < 0.001$ compared with NT control) (Figure 6b).

NOD/SCID mice were then inoculated with the transduced polyclonal (LV/LNGFRΔTmpk) or NT Raji cells (Figure 6c). Starting 4 days after inoculation, mice received twice-daily injections for 2 weeks of AZT (17.1 mg kg^{-1} per injection) or the phosphate-buffered saline (PBS) carrier. For the control groups, tumorigenic activity, as evidenced by total hind-limb paralysis (with subsequent euthanasia) in all mice, manifested at 18–25 days post inoculation with a median survival time of ~20 days. Concerning the experimental group, mice that received transduced Raji cells with AZT treatment showed a significant increase in survival ($P < 0.001$) compared with the PBS treatment group, with median survival of 26 days (Figure 6c).

At the time of paralysis/euthanization, peripheral blood and bone marrow (BM) were harvested and analyzed for the presence of the Raji cells. Peripheral blood showed little or no Raji cells in circulation (<1%) (data not shown). As expected, BM obtained from the control groups showed a high prevalence of transduced (human CD19$^+$LNGFR$^+$) or NT (human CD19$^+$) Raji cells of 23.5% for both groups ranging from 8.0 to 80.0% and 5.5 to 40.9%, respectively. In contrast, healthy mice euthanized from the experimental group (LNGFRΔTmpk + AZT) within this same time-frame (19–21 days post inoculation) only showed a median engraftment of leukemic cells of 6.6% (ranging from 0.2 to 9.2%; Figure 6d). Remarkably, one mouse in the experimental group showed only 0.2% CD19-positive cells in the BM, suggesting that the AZT at this dose had effectively eradicated the transduced cells in that case.

Specific enrichment and AZT-mediated killing of LV/LNGFRΔTmpk-transduced primary human T cells

To investigate the efficacy of our novel LNGFRΔTmpk safety cassette for prevention of potential serious adverse events (that is, graft-versus-host disease) associated with T-cell immunotherapies, we transduced and expanded primary human T cells from peripheral blood collected from a healthy donor, using a protocol analogous to current clinical preparation of primary human T cells for adoptive immunotherapy or chimeric antigen receptor immunotherapy. Expanded T cells were transduced with LV/LNGFRΔTmpk at an MOI of 100. The transduction process did not affect the frequency of CD3 expression, and ~44% of T cells expressed LNGFR after a single transduction (Figures 7a and b). Cell sorting by immunomagnetic selection for LNGFR further enriched for T cells expressing the safety cassette to ~92% purity (Figure 7b); these enriched T cells can undergo multiple rounds of sorting to achieve even higher purities. To determine the killing efficiency of LNGFRΔTmpk in transduced T cells, unsorted, transduced T cells were treated with AZT. Comparison of LNGFRΔTmpk$^+$ and LNGFRΔTmpk$^-$ cells within the same culture shows that LNGFRΔTmpk$^+$ cells were killed twofold more effectively than non-transduced T cells (Figure 7c), thus showing the clinical feasibility of the LNGFRΔTmpk cassette as an added safety measure for T cell-based immunotherapies.

Therapeutic LV targeting Fabry disease generates both enzyme correction in transduced cells and sensitivity to AZT

In 'proof-of-principle' studies, a novel LV designed for amelioration of Fabry disease was also endowed with the CFCGT safety cassette. To evaluate if the LV/LNGFRΔTmpk-IRES-COα-gal A we engineered could provide enzymatic correction, a human Fabry B-cell line was transduced a single time at an MOI of 100. Cells were found to be ~15% positive for LNGFRΔ or ~70% positive for control enGFP expression (data not shown). Transduced Fabry B cells were enriched by FACS and found to be >98% positive for LNGFR expression (Figure 8a). When the α-gal A enzyme activity was assayed on lysates from the enriched cells, we found that human Fabry B cells showed fully restored enzyme activity compared with NT or LNGFRΔTmpk Fabry B cells ($P < 0.001$); in fact a nearly twofold activity increase over that seen in normal B cells (Figure 8b). In addition, *in-vitro* cytotoxicity assays showed that the transduced polyclonal Fabry B cells were selectively sensitive to AZT in a similar dose-dependent manner as seen above with significant cytotoxicity observed at concentrations as low as 0.1 μM AZT ($P < 0.001$ compared with NT control; Figure 8c). To demonstrate clinical applicability of this novel therapeutic/safety vector for therapeutic amelioration of Fabry disease, we transduced human CD34$^+$ cells enriched from peripheral blood

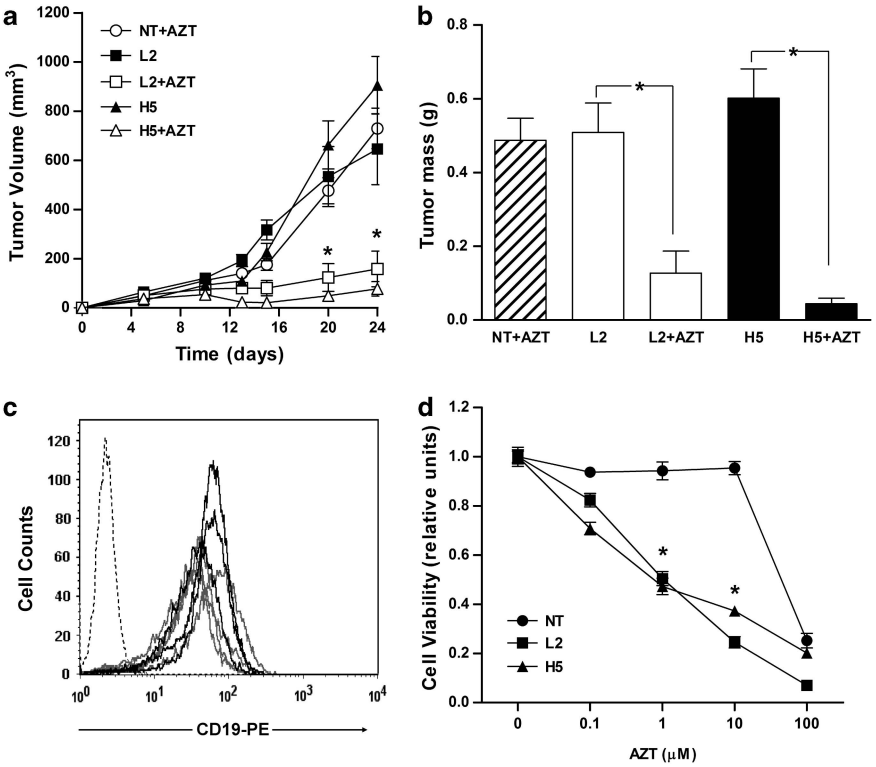

Figure 5. *In-vivo* tumor killing mediated by AZT. NOD/SCID mice were injected subcutaneously with 1×10^7 cells of either the NT or the low (L2) and high (H5) CD19 expressing clones in the left and right dorsal flanks, respectively. Starting 1 day after the cell injection, the mice received daily intraperitoneal injections of AZT (17.1 mg kg^{-1} per day) for 2 weeks and tumor size was monitored. (**a**) Subcutaneous tumor growth in NOD/SCID mice. Data are mean measurements ± s.e.m., $n = 5-11$, $^*P < 0.005$. (**b**) Tumor weight (grams) on day 24. Data are mean measurements ± s.e.m., $^*P < 0.005$. (**c**) Flow cytometry analysis of extracted residual tumor-derived K562 cells from independent mice. (**d**) Tumor-derived K562 cells sensitivity to AZT measured by quadruplicates by the MTS proliferation assay following 4 days in the presence or absence of different AZT concentrations. Data are mean measurements ± s.d., $n = 3$, $^*P < 0.001$ compared with NT control. The statistical significance between groups was calculated by the two-tailed, Student's *t*-test, $^*P < 0.001$ compared with NT control. NT, non-transduced.

apheresis harvests. Using a clinically relevant magnetic enrichment protocol, $CD34^+$ cells were isolated with a >95% purity (Figure 9a). Enriched $CD34^+$ cells were transduced a single time with LV/LNGFRΔTmpk-IRES-COα-gal A at an MOI of 100 to achieve a transduction efficiency of ~74% (Figure 9b). Secreted α-gal A activity was determined from culture supernatants from enriched $CD34^+$ cells collected from four individual normal donors with and without transduction of LV/LNGFRΔTmpk-IRES-COα-gal A. From six individual transductions of enriched $CD34^+$ cells, 3–8-fold increases in supernatant α-gal A activity were detected in LV/LNGFRΔTmpk-IRES-COα-gal A-transduced cells (Figure 9c). To further evaluate the translational applicability of this novel therapeutic/safety vector, we transduced BM-derived $CD34^+$ Fabry patient cells and analyzed the efficiency of transduction by flow cytometry 5 days later. As shown in Figures 9d and e, with an MOI of 100 it was possible to get ~50% $LNGFR^+$ cells, reaching ~65% with an MOI of 200. No significant differences were observed in the colony-generating capacity of the transduced Fabry patient $CD34^+$ cells in comparison with the NT controls (Figure 9f). These initial results on this key target cell population have important clinical implications for future therapy of Fabry disease.

DISCUSSION

Cell-fate control (aka 'suicide') gene therapy has a myriad of potential applications in the clinic. Such applications include bystander killing of solid tumors, resolution of graft-versus-host disease in therapies based on modified T cells, clearance of modified embryonic or induced-Pluripotent Stem cells if teratomas develop, as well as inclusion as safety components in clinical protocols involving integrating viral vectors. Here, we have expanded on our previous human Tmpk/AZT system,[15] which already overcame many of the limitations of existing suicide genes, such as immunogenicity of the transgene, poor enzyme kinetics and unfavorable prodrug utilization. To enhance applicability and portability, we have created two novel fusion Tmpk variant enzymes utilizing truncated human cell-surface markers, CD19 and LNGFR. Both fusion constructs were stably expressed and retained their Tmpk/AZT-mediated killing functionalities. Importantly, the fused cell-surface markers and kinases are now expressed at an enforced one-to-one level. Use of such cell-surface molecules will not only allow for enrichment and tracking but also will enable a secondary cell killing approach.[18] For instance, phase I clinical studies have been conducted using a CD19-directed antibody conjugated to the Ricin A toxin.[23,24] Along these lines, combination therapies of CD19-immunotoxin and AZT may show even greater eradication of transduced cells.

We demonstrated that these novel cell-fate control safety cassettes we generated can be used to control the survival of transduced cells both *in vitro* and *in vivo*. Indeed, our xenograft-NOD/SCID tumor model showed significant suppression of tumor growth (Figures 5a and b). Of particular importance, we further showed that only 1 vector copy per cell with relatively low transgene expression was sufficient to mediate Tmpk/AZT killing. Worth noting as well is that clones H5 and L2 show a different

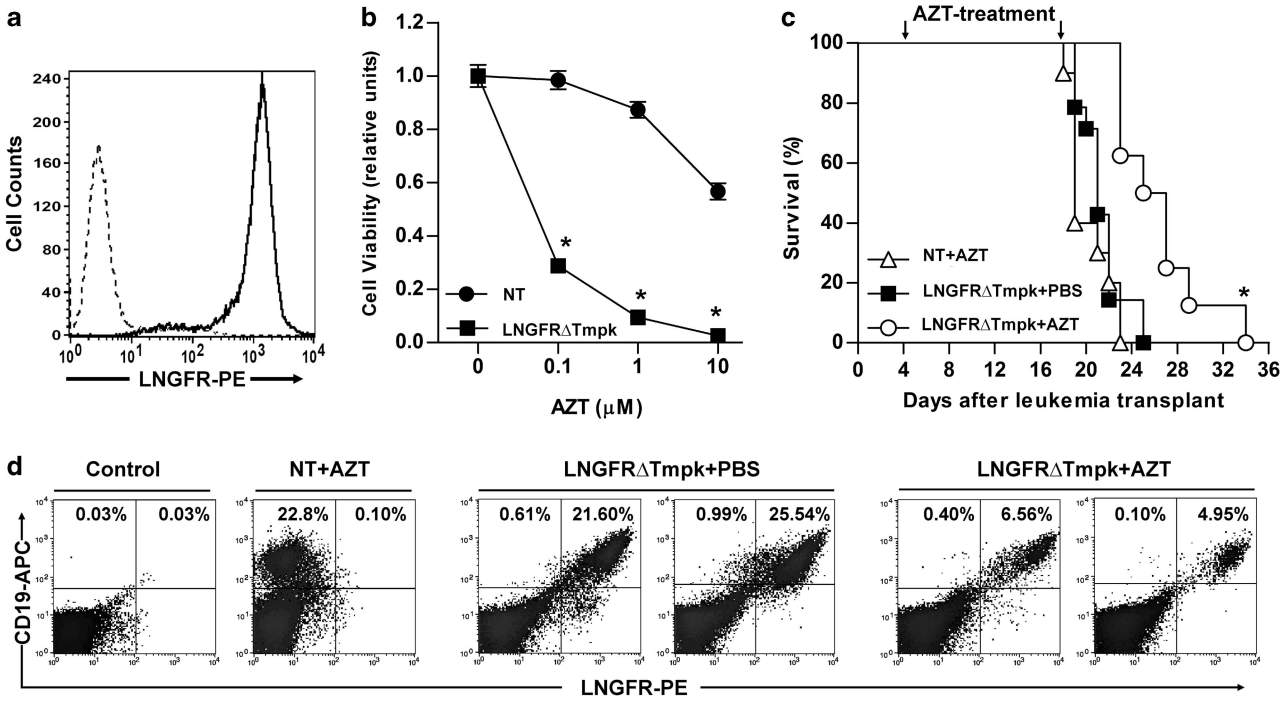

Figure 6. *In-vivo* killing of transduced (LV/LNGFRΔTmpk) and NT Raji cells in a disseminated leukemia-lymphoma model. (**a**) Flow cytometry analysis of NT and transduced (LV/LNGFRΔTmpk) Raji cells before cell transplantation. (**b**) Sensitivity of NT or transduced Raji cells to AZT measured by MTS assay following 4 days of AZT treatment. Data are mean ± s.d. ($n = 4$). The statistical significance between groups was calculated by the two-tailed, Student's *t*-test, $^*P < 0.001$ compared with NT control. (**c**) Kaplan–Meier survival curve of NOD/SCID mice transplanted with transduced and NT Raji cells. Starting 4 days after the cell injection, the mice received twice-daily intraperitoneal injections of AZT (17.1 mg kg^{-1}) during 2 weeks. The animals were monitored daily and euthanized upon appearance of symptoms. The statistical significance between groups was calculated by Mantel–Cox test, $P < 0.001$ compared with PBS group. (**d**) BM engraftment of Raji cells at the time of euthanasia. Representative dot plots from each experimental group are shown.

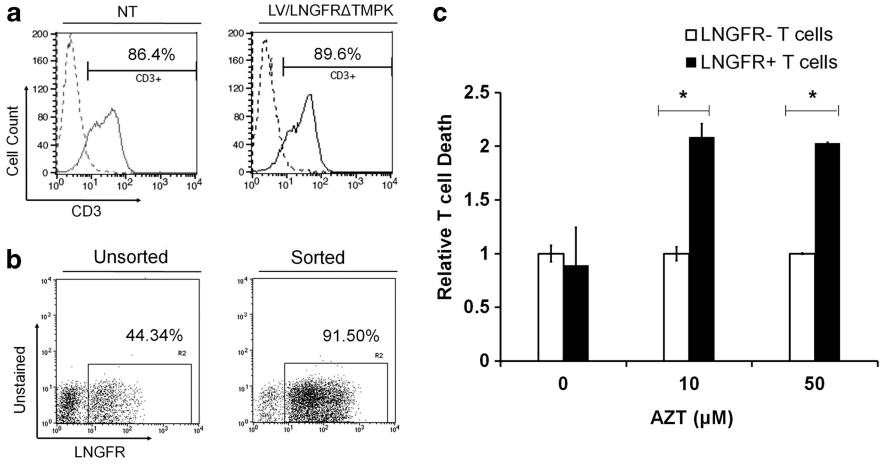

Figure 7. Primary human T cells transduced with LV/LNGFRΔTmpk can be enriched and specifically killed by AZT. (**a**) Representative histograms showing CD3 expression on primary human T cells expanded from peripheral blood mononuclear cell and transduced with LV/LNGFRΔTmpk. (**b**) Representative dots plots showing LNGFR expression on transduced T cells 4 days post-transduction before and after immunomagnetic enrichment with anti-LNGFR microbeads. (**c**) Transduced T cells were treated with AZT at the indicated concentrations for 4 days. LNGFRΔTmpk-expressing T cells displayed a twofold increase in cell death as determined by flow cytometry analysis of Annexin V and propidium iodide staining (mean ± s.d.). The statistical significance between groups was calculated by the two-tailed, Student's *t*-test, $^*P < 0.01$ compared with non-transduced controls.

level of transgene expression in spite of the similar copy number (Figure 3); this is probably due to different integration sites or epigenetic status of the surrounding chromatin. One previous shortcoming of the older-generation HSV-TK/GCV system was that the HSV-TK cDNA contained active cryptic splice sites, resulting in a fraction of up to 5% of transduced target cells insensitive to drug-mediated killing.[6] Here, we confirmed that the remaining tumor cells were not escape mutants or evading drug selection, as remaining residual tumor cells were sensitive to AZT *in vitro* (Figures 5c and d). This suggests that the drug treatment regimen in this case may not have been aggressive enough to completely eradicate all of the infused tumor cells. However, this result is

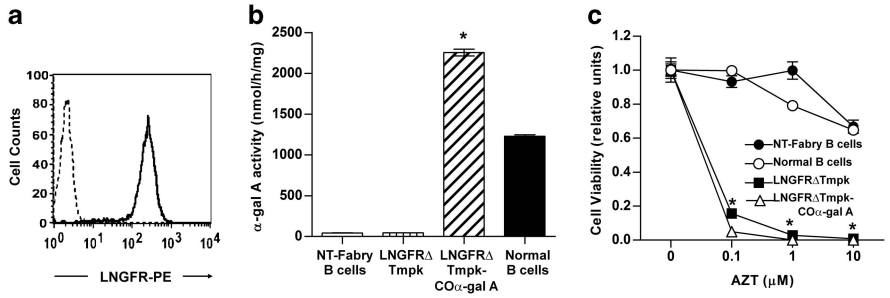

Figure 8. Fabry B cells transduced with therapeutic LV/LNGFRΔTmpk-IRES-COα-gal A. (**a**) Flow cytometry analysis of transduced and enriched Fabry B cells. (**b**) Intracellular α-gal A enzyme activity of transduced Fabry and normal B cells measured by a microtiter plate-based fluorometric assay. Data are mean ± s.e.m. ($n = 3$). The statistical significance between groups was calculated by the two-tailed, Student's *t*-test, $*P < 0.001$ compared with NT control. (**c**) Sensitivity of NT or transduced B cell line to AZT measured by MTS assay following 4 days of AZT treatment. Data are mean ± s.e.m. ($n = 4$). The statistical significance between groups was calculated by the two-tailed, Student's *t*-test, $*P < 0.001$ compared with NT control.

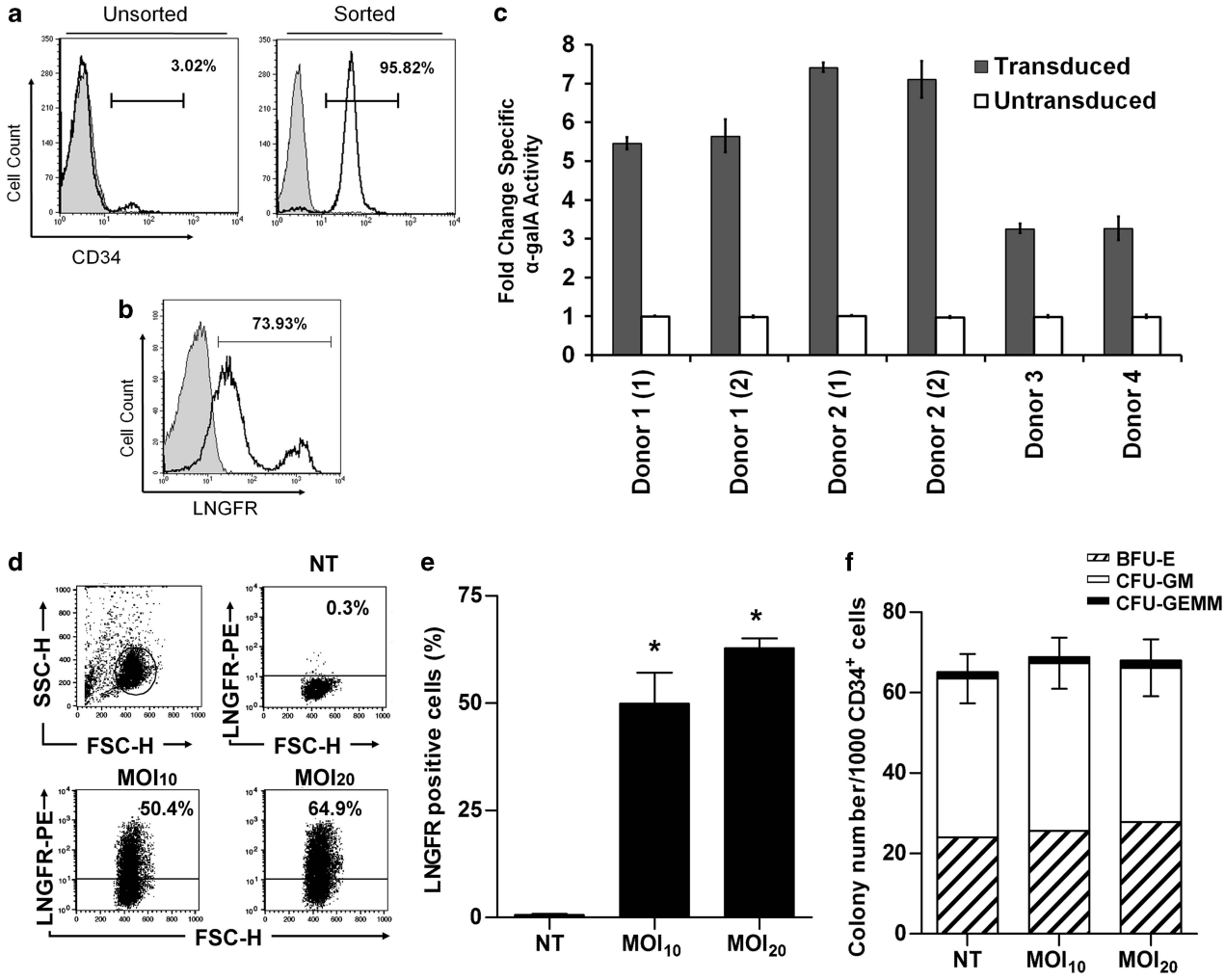

Figure 9. Increased α-gal A secretion and normal clonogenic capacity in LV/LNGFRΔTmpk-IRES-COαgalA-transduced human hematopoietic precursors cells. (**a**) Representative histogram showing enrichment of human $CD34^+$ cells from apheresis harvests by positive immunomagnetic-based selection. (**b**) Representative histogram showing efficient transduction of enriched $CD34^+$ cells with LV/LNGFRΔTmpk-IRES-COα-gal A at an MOI of 100. (**c**) Fold changes in secreted α-gal A activity of transduced $CD34^+$ cells from four individual donors (triplicate measurements ± s.d.). (**d**) Representative dot plots showing efficiency of transduction of Fabry patient BM-derived $CD34^+$ cells and (**e**) percentage of $LNGFR^+$ cells at 5 days after transduction of $CD34^+$ Fabry patient cells (mean ± s.d.; $n = 3$). The statistical significance between groups was calculated by the two-tailed, Student's *t*-test, $*P < 0.001$ compared with NT control. (**f**) Total number and types of colonies obtained from transduced and non-transduced $CD34^+$ cells after 12 days in culture. Values are expressed as means ± s.d. of three independent experiments performed in duplicate.

quite notable considering the low drug dose of 17.1 mg kg^{-1} per day that was used, compared with data from mice treated with AZT at 270 mg kg^{-1} per day for 15 days, which only exhibited marginal toxicity.[25]

In our other *in-vivo* model, we found a significant increase in the survival of animals harboring the transduced polyclonal Raji cells following 2 weeks of AZT treatment (Figure 6c). Yet, AZT treatment did not fully prevent animals from succumbing to the disorder. The aggressiveness of this leukemia-lymphoma model and a less than-optimal drug-dosing regimen may have contributed to this. In the clinic, to prevent fetal transmission of HIV, HIV$^+$ pregnant women are treated orally with 100 mg of drug, five times per day. At labor time, the treatment is reinforced with 2 mg kg^{-1} during the first hour followed by continuous infusion of 1 mg kg^{-1} per hour until clamping of the umbilical cord. The reason behind this aggressive and continuous dosing of AZT is due to its short plasma half-life, which is as low as 30 min.[22] Although the short half-life or desirable frequency of administration of AZT to mice was a challenge in these aggressive disease studies, this would likely not to be problematic in humans given that AZT is already commonly used in the clinic either as a continuous i.v. infusion or is given in multiple oral doses. Along these lines, we believe that enhancing the AZT half-life through drug modification may further improve our cell-fate control system. This work is already under investigation for enhancing the efficacy of this drug for treatment of HIV.[26–28] Another major consideration is the biodistribution of the prodrug versus accessibility of privileged sites in the animal. The cells used in these leukemia-lymphoma models have been selected over generations to be very aggressive. They also migrate to the regions that are less accessible to the drug, such as the spinal cord and brain.[29,30] These models may thus be too stringent to study a realistic onset of leukemia in a gene therapy context.

Our laboratory is currently transitioning to using these safety cassettes in gene therapy approaches for inherited disorders. One of our present applications of these cell-fate control safety cassettes is to safeguard against insertional oncogenesis in LV-mediated therapy for Fabry disease. To this end, a novel LV that engineers the expression of LNGFRΔTmpk along with an intact human COα-gal A cDNA was constructed in this present study. Transduction of human Fabry B cells and human CD34$^+$ cells with this LV resulted in supranormal levels of α-gal A expression and activity (Figures 8b and 9c). Having these supranormal levels of α-gal A is desirable to facilitate metabolic cooperativity or cross-correction. Of particular importance, strong overexpression of α-gal A is well tolerated, as transgenic mice with α-gal A levels up to 11 080-fold higher than normal displayed no associated toxicity.[31] These data suggest that α-gal A downstream of an IRES element may be sufficient to provide enzymatic correction in Fabry disease, in part owing to the premise that as little as 5–10% of residual enzyme activity seems to be sufficient to prevent clinical accumulation of glycosphingolipids.[32] Our laboratory is currently in preclinical validation of this LV for the treatment of Fabry disease. Although future work is currently ongoing to evaluate this therapeutic vector for treatment of Fabry disease, these present results themselves are encouraging. Even with very limited Fabry patient CD34$^+$ cells, we showed high expression levels of LNGFR cell-surface marker on transduced cells, and transduced cells retained normal colony-generating capacity when compared with the NT controls. Furthermore, we demonstrated high levels of secreted α-gal A in LV/LNGFRΔTmpk-IRES-COα-gal A-transduced CD34$^+$ cells. Treatment of Fabry disease is only one of the many possible applications of this system. We have also demonstrated effective selection and AZT-mediated killing in human primary T cells using the LNGFRΔTmpk element following a clinically analogous expansion and selection protocol. These safety cassettes are already incorporated into some of our adoptive immunotherapy constructs and we have recently demonstrated the successful use of the CD19ΔTmpk cassette for cell eradication in an adoptive immunotherapy approach using T cells engineered to also express PDL1.[33] These results highlight the clinical feasibility of these fusion cassettes in both therapeutic gene therapy and cell-based immunotherapy scenarios.

MATERIALS AND METHODS

Materials

Roswell Park Memorial Institute (RPMI-1640), Dulbecco's Modified Eagle's Medium, AZT and collagenase II were from Sigma (Oakville, ON, USA). Fetal bovine serum was from PAA (Toronto, ON, Canada). Glutamine, penicillin and streptomycin were from Invitrogen (Carlsbad, CA, USA). KOD Hot Start DNA Polymerase was from Toyobo (Osaka, Japan). The TA cloning vector pGEM-T Easy was from Promega (Madison, WI, USA). Antibodies used for flow cytometry were PE-conjugated anti-human CD19 monoclonal antibody (anti-CD19-PE), anti-CD19-APC and CD271-PE (all from BD Biosciences, San Jose, CA, USA).

Construction of the CD19ΔTmpk fusion LV

The cDNA for both CD19Δ and TmpkF105Y was amplified from a previously constructed shuttle vector pSV-TmpkF105Y-IRES-CD19Δ[15] and ligated into the TA cloning vector pGEM-T. To generate the CD19ΔTmpkF105Y fusion cassette and to facilitate the proper folding of the both proteins, a six amino-acid linker peptide (Ala-Gly-Gly-Ala-Ala-Gly) was inserted between both construct components. The CD19ΔTmpkF105Y cDNA sequence was then excised and subcloned into the self-inactivating (SIN) HIV-based lentiviral backbone (pDY'cPPT-EF1α-woodchuck hepatitis virus post-transcriptional regulatory element (WPRE)) previously generated in our laboratory from the pHR'.cPPT.EF-1α.EGFP.WPRE.SIN.[19] Briefly, in an effort to reduce the size of the transfer vector and to facilitate future subcloning procedures, non-essential elements of the original transfer vector backbone and long terminal repeat sequences were deleted via PCR mutagenesis. The PCR-amplified fragment was subsequently subcloned into the pGEM vector and the newly engineered transfer vector was then denoted as pDY.cPPT.EF-1α.EGFP.WPRE.SIN. The fidelity of the final construct was confirmed by restriction enzyme digests and bidirectional DNA sequencing.

Construction of the LNGFRΔTmpk fusion LV

A CO cDNA sequence of human LNGFRΔTmpk was synthesized by GenScript (Piscataway, NJ, USA). The human LNGFR cDNA sequence was truncated in the intracellular domain. The entire CO LNGFRΔTmpkF105Y sequence was synthesized with a 5′ flanking *Asc*I site and a Kozak consensus sequence along with a 3′ *Bam*HI site. The COLNGFRΔTmpkF105Y sequence was then subcloned into the SIN HIV-based lentiviral backbone (pDY′ EF1α-WPRE). The fidelity of the final construct was confirmed by restriction enzyme digests and bidirectional DNA sequencing.

Construction of the LNGFRΔTmpk-IRES-COαgalA LV

A CO cDNA sequence of human α-gal A gene was synthesized by DNA2.0 (Menlo Park, CA, USA). The COα-gal A cDNA was amplified by PCR and subcloned into a TA cloning vector, excised and used to replace the eGFP element from a pDIG-CMV-DsRed-IRES-eGFP vector previously constructed in our laboratory (unpublished results). Then, the IRES-COα-gal A component was amplified, digested and ligated into the *Bam*HI site downstream of the LNGFRΔTmpk element of the pDY-LNGFRΔTmpk plasmid. The fidelity of the final construct was confirmed as above.

Cell culture

HEK 293T cells (human embryonic kidney cells) were cultured in Dulbecco's Modified Eagle's Media while K562 cells (human erythroid leukemia cells), Raji cells (Burkitt's human lymphoma B cells) and a Fabry patient-derived B-cell line[34] were cultured in RPMI-1640 media. Both media were supplemented with 10% fetal bovine serum, 2 mM glutamine,

100 U ml^{-1} penicillin and 100 mg ml^{-1} streptomycin. All cells were maintained in a humidified incubator at 37 °C with 5% CO_2.

Fabry BM samples and a peripheral blood apheresis harvest were obtained from Fabry patients and normal donors, respectively, following the protocols approved by the Research Ethics Board at the McMaster University (Hamilton, ON, Canada) after obtaining informed consent. Peripheral blood mononuclear cells were isolated from apheresis harvests by Ficoll-paque PLUS (GE Amersham, Buckinghamshire, UK) density gradient. CD34$^+$ cells were enriched from total mononuclear cells by positive immunomagnetic separation in accordance with the manufacturer's recommendations (Miltenyi Biotech, Auburn, CA, USA). CD34$^+$ cells were cultured in Stem Span medium (Stem Cell Technologies, Vancouver, BC, Canada) in the presence of 20 ng ml^{-1} human interleukin-6, 50 ng ml^{-1} human Flt3 Ligand (Flt3-L), 50 ng ml^{-1} human thrombopoietin and 100 ng ml^{-1} human stem cell factor (all growth factors were purchased from R&D Systems, Minneapolis, MN, USA) and incubated at 37 °C/5% CO_2. Clonogenic assays were performed 24 h after transduction following the manufacturer's recommendations (MethoCult; Stem Cell Technologies). The use of these cells *in vitro* was approved by the Research Ethics Board of the University Health Network.

Culture and enrichment of primary T lymphocytes

Human primary T lymphocytes were expanded from Ficoll-paque PLUS isolation of peripheral blood mononuclear cell cultured at 1×10^6 cells per ml in X-Vivo 20 (Lonza, Walkersville, MD, USA) supplemented with 5% inactivated human AB serum (Invitrogen). The T cells were activated using anti-CD3/CD28 beads (three beads per cell) and 20 IU ml^{-1} of recombinant human interleukin-2 (AbD Serotec, Raleigh, NC, USA) in the presence of 1 μM rapamycin (Sigma). T cells were infected at 48 h of culture with concentrated LV at an approximate functional MOI of 100. Transduced primary T lymphocytes were enriched by indirect immunomagnetic selection for LNGFR following the manufacturer's instructions (Miltenyi Biotec).

Preparation of high-titer LV and functional titer analyses

Vesicular stomatitis virus glycoprotein-pseudotyped LVs including control LV/enGFP[15] were generated by transient co-transfection of 293T cells with a three-plasmid system (the transfer construct, the packaging plasmid pCMVΔR8.91 and the vesicular stomatitis virus glycoprotein envelope encoding plasmid pMD.G) using PEI transfection (Sigma). Viral supernatants were harvested at 48 and 72 h after transfection, passed through a 0.45-μM filter (Nalgene, Rochester, NY, USA), and ultracentrifuged at 50 000 *g* for 120 min at 4 °C. The concentrated viral pellets were resuspended in 2% bovine serum albumin in 1 × PBS and stored in aliquots at −80 °C. Functional viral titers were determined by serial diluting the concentrated LV and transducing naive 293T cells. Transgene expression in such transduced cells was assessed 72 h after infection by flow cytometry. An FACS Calibur flow cytometer (BD Biosciences) and CellQuest software (BD Biosciences) were used for all cell analyses.

Transduction and clonally derived cell lines

Cell lines were infected with concentrated LV stocks for 16 h in the presence of 8 μg ml^{-1} protamine sulfate. Transgene expression was assessed 72 h after transduction. Transduced cells were also enriched by FACS. For these studies, transduced cells were stained as above and sorted using an MoFlo high-performance flow cytometer (Dako Canada Inc., Burlington, ON, Canada). To obtain clonally derived cell lines, sorted K562 cells were plated in Nyco plates at densities of 0.3 cells per well. Only wells containing a single cell were expanded.

Quantification of CD19ΔTmpk expression

Quantification of CD19 cell-surface molecule expression on K562 single cell-derived clones was performed using an ABC flow cytometry quantification kit as per the manufacturers instructions (Quantum Simply Cellular, Bangs Laboratory Inc., Fishers, IN, USA). The Quantum Simply Cellular beads and K562 clones were labeled with the anti-CD19-PE monoclonal antibody. By plotting each microsphere population's fluorescence intensity versus its assigned ABC value, a standard ABC curve was generated. A QuickCal analysis Microsoft Excel template (Bangs Labs, Fishers, IN, USA) was used to determine the CD19 ABC of the K562 clones based on the ABC/MFI (mean fluorescence intensity) of the standard beads.

Analysis of transgene expression by western blot

In all, 20 μg of total cell lysates was resolved by 12% SDS-PAGE and transferred onto a PVDF membrane (Millipore, Billerica, MA, USA). Membranes were blocked overnight at 4 °C using 5% w/v non-fat dry milk in PBS-T (0.1% Tween-20 v/v in PBS). A 1:5000 dilution of serum from a rabbit immunized against human Tmpk in 5% non-fat dry milk was applied to the membrane and incubated at room temperature for 3 h.[15] After washing in PBS-T, a secondary goat anti-rabbit IgG antibody conjugated to horseradish peroxidase (Santa Cruz Biotechnology, Santa Cruz, CA, USA), diluted 1:10 000 in 5% non-fat dry milk was added. Proteins were visualized using Western Lightning Chemiluminescence Reagent Plus (Perkin-Elmer, Woodbridge, ON, USA). Protein loading amounts were confirmed with a monoclonal anti-β-actin primary antibody (Chemicon International, Billerica, MA, USA).

Vector copy number assessed by quantitative real-time PCR

Genomic DNA was isolated from transduced K562 clones using the Gentra Puregene Blood kit (Qiagen, Valencia, CA, USA), as per the manufacturer's instructions. Quantitative real-time PCR for the WPRE element in the LV and β-actin control was performed for integrated provirus as before[35] using the Corbett Research Rotor Gene RG3000 thermocycler (Concorde, NSW, Australia). A no-template negative control was included; moreover, each reaction was performed in triplicate, and mean Cycle Threshold values were calculated. A standard curve to determine vector copy number was created using serial dilutions of genomic DNA from a 293T-based cell line we previously generated that contains one integrated provirus.[35]

Determination of sensitivity of transduced cells to AZT

Cells were seeded at a density of 5–10 × 10^{6}cells per ml and treated daily with increasing concentrations of AZT for 4 consecutive days. On day 7, cell viability was determined using the Cell Titer 96 Aqueous One Solution Cell Proliferation Assay kit (Promega) as per the manufacturer's specifications. Cell viability was calculated by normalizing absorbance values at each concentration of AZT against its respective non-treated value for each group. Standard deviation is representative of normalized absorbance values performed in quadruplicates, and statistical significance between groups was calculated by the two-tailed, Student's *t*-test.

For evaluation of the induction of apoptosis, cells were treated with different AZT concentrations during 3 days. On day 4, the cells were stained with FITC Annexin V (BD Biosciences) and propidium iodide and flow cytometry was performed. Data obtained were normalized by dividing results from the AZT-treated cells in each group by the results obtained without AZT treatment.

Subcutaneous tumor model of K562 cells in NOD/SCID mice

All animal experimental procedures followed a protocol approved by the Animal Care Committee of the University Health Network (Toronto, ON, Canada). NOD/SCID mice (females, 6–10-week old) were bred in a pathogen-free environment and were maintained at the Animal Resource Centre at the Princess Margaret Hospital (Toronto, ON, Canada). All mice received 1×10^7 cells per flank injected in 200 μl of 1 × PBS. Experimental groups consisted of transduced K562 clone H5 (CD19ΔTmpk^{HIGH}) cells injected subcutaneously into the right dorsal flank, with the K562 clone L2 (CD19ΔTmpk^{LOW}) injected subcutaneously into the left dorsal flank of the same mouse. Control groups consisted of NT K562 cells injected similarly. One day after injection of cells, half of the animals from the experimental group began receiving daily AZT, administered intraperitoneally at a dose of 17.1 mg kg^{-1} per day for 14 days, while the rest remained untreated (control). Tumor growth was monitored for 21 days post injection of cells;

tumor volume was calculated as $L \times W \times H$ (in mm^3). At the time of euthanasia, tumors were extracted (if any were present) and weighed (grams). K562 tumors were further processed by cutting the tumor into multiple pieces and incubation with 0.05% w/v collagenase for 1 h. This cell suspension was then passed through a cell strainer and cultured for expansion. Data are presented as the mean ± s.e.m. Statistical significance between groups was calculated by the two-tailed Student's *t*-test.

Disseminated leukemia-lymphoma model using Raji cells in NOD/SCID mice

Experimental groups consisted of NOD/SCID mice receiving Raji cells transduced with LV/pDY-LNGFRΔTmpk and NT controls. At the time of transplantation, all mice received 2×10^6 cells in 200 µl of 1 × PBS via tail vein injection. Four days after injection of cells, half of the LNGFRΔTmpk group of mice and the entire population of NT Raji-transplanted mice received twice-daily intraperitoneal injections of AZT for 14 days at a concentration of 17.1 mg kg^{-1} per injection. Animals were monitored daily for signs of disease and killed immediately if hind-limb paralysis occurred. Survival time (= paralysis time) was used as the primary endpoint for evaluation.

α-Galactosidase an enzyme-specific activity assay

α-Gal A activity was measured by a microtiter plate-based fluorometric assay as using the substrate 4-methylumbelliferyl-α-D-glucopyranoside (Research Products International, Mt. Prospect, IL, USA) as described previously.[19,36] Reactions were incubated for 2 h at 37 °C and stopped by stop solution (1.1 M glycine and 0.1 M NaOH). Samples were measured in an MFX Microtiter Plate Fluorometer (Dynex, Chantilly, VA, USA). Readings were normalized against protein concentrations determined by the DC Protein Assay (Bio-Rad, Hercules, CA, USA). Enzyme activity was reported as nmol per hour per mg protein. Error bars are standard deviation of reactions performed in triplicate. Statistical differences were calculated by the two-tailed, Student's *t*-test.

CONFLICT OF INTEREST

The authors declare no conflict of interest.

ACKNOWLEDGEMENTS

We would like to especially thank the Fabry patients who donated bone marrow to facilitate these studies. This research was funded by a research operating grant from the Canadian Institutes of Health Research to Dr JA Medin. Funding for AN was provided by the CIHR Training Program in Regenerative Medicine (TPRM).

REFERENCES

1 Morgan RA, Yang JC, Kitano M, Dudley ME, Laurencot CM, Rosenberg SA. Case report of a serious adverse event following the administration of T cells transduced with a chimeric antigen receptor recognizing ERBB2. *Mol Ther* 2010; **18**: 843 - 851.
2 Brentjens R, Yeh R, Bernal Y, Riviere I, Sadelain M. Treatment of chronic lymphocytic leukemia with genetically targeted autologous T cells: case report of an unforeseen adverse event in a phase I clinical trial. *Mol Ther* 2010; **18**: 666 - 668.
3 Bonini C, Ferrari G, Verzeletti S, Servida P, Zappone E, Ruggieri L *et al.* HSV-TK gene transfer into donor lymphocytes for control of allogeneic graft-versus-leukemia. *Science* 1997; **276**: 1719 - 1724.
4 Tiberghien P, Ferrand C, Lioure B, Milpied N, Angonin R, Deconinck E *et al.* Administration of herpes simplex-thymidine kinase-expressing donor T cells with a T-cell-depleted allogeneic marrow graft. *Blood* 2001; **97**: 63 - 72.
5 Berger C, Flowers ME, Warren EH, Riddell SR. Analysis of transgene-specific immune responses that limit the *in vivo* persistence of adoptively transferred HSV-TK-modified donor T cells after allogeneic hematopoietic cell transplantation. *Blood* 2006; **107**: 2294 - 2302.
6 Garin MI, Garrett E, Tiberghien P, Apperley JF, Chalmers D, Melo JV *et al.* Molecular mechanism for ganciclovir resistance in human T lymphocytes transduced with retroviral vectors carrying the herpes simplex virus thymidine kinase gene. *Blood* 2001; **97**: 122 - 129.
7 Deschamps M, Mercier-Lethondal P, Certoux JM, Henry C, Lioure B, Pagneux C *et al.* Deletions within the HSV-tk transgene in long-lasting circulating gene-modified T cells infused with a hematopoietic graft. *Blood* 2007; **110**: 3842 - 3852.
8 Blumenthal M, Skelton D, Pepper KA, Jahn T, Methangkool E, Kohn DB. Effective suicide gene therapy for leukemia in a model of insertional oncogenesis in mice. *Mol Ther* 2007; **15**: 183 - 192.
9 Willmon CL, Krabbenhoft E, Black ME. A guanylate kinase/HSV-1 thymidine kinase fusion protein enhances prodrug-mediated cell killing. *Gene Therapy* 2006; **13**: 1309 - 1312.
10 Black ME, Kokoris MS, Sabo P. Herpes simplex virus-1 thymidine kinase mutants created by semi-random sequence mutagenesis improve prodrug-mediated tumor cell killing. *Cancer Res* 2001; **61**: 3022 - 3026.
11 Ardiani A, Sanchez-Bonilla M, Black ME. Fusion enzymes containing HSV-1 thymidine kinase mutants and guanylate kinase enhance prodrug sensitivity *in vitro* and *in vivo*. *Cancer Gene Ther* 2010; **17**: 86 - 96.
12 Akyurek LM, Nallamshetty S, Aoki K, San H, Yang ZY, Nabel GJ *et al.* Coexpression of guanylate kinase with thymidine kinase enhances prodrug cell killing *in vitro* and suppresses vascular smooth muscle cell proliferation *in vivo*. *Mol Ther* 2001; **3**: 779 - 786.
13 Stasi AD, Tey SK, Fujita Y, Cruz R, Martinez C, Kennedy-Nasser A *et al.* CASPALLO: phase I clinical trial of allodepleted T cells transduced with inducible caspase 9 suicide gene after haploidentical stem cell transplantation. *Mol Ther* 2010; **18**: S110.
14 Tey SK, Dotti G, Rooney CM, Heslop HE, Brenner MK. Inducible caspase 9 suicide gene to improve the safety of allodepleted T cells after haploidentical stem cell transplantation. *Biol Blood Marrow Transplant* 2007; **13**: 913 - 924.
15 Sato T, Neschadim A, Konrad M, Fowler DH, Lavie A, Medin JA. Engineered human tmpk/AZT as a novel enzyme/prodrug axis for suicide gene therapy. *Mol Ther* 2007; **15**: 962 - 970.
16 Brundiers R, Lavie A, Veit T, Reinstein J, Schlichting I, Ostermann N *et al.* Modifying human thymidylate kinase to potentiate azidothymidine activation. *J Biol Chem* 1999; **274**: 35289 - 35292.
17 Ostermann N, Lavie A, Padiyar S, Brundiers R, Veit T, Reinstein J *et al.* Potentiating AZT activation: structures of wild-type and mutant human thymidylate kinase suggest reasons for the mutants' improved kinetics with the HIV prodrug metabolite AZTMP. *J Mol Biol* 2000; **304**: 43 - 53.
18 Ramsubir S, Yoshimitsu M, Medin JA. Anti-CD25 targeted killing of bicistronically transduced cells: a novel safety mechanism against retroviral genotoxicity. *Mol Ther* 2007; **15**: 1174 - 1181.
19 Yoshimitsu M, Higuchi K, Ramsubir S, Nonaka T, Rasaiah VI, Siatskas C *et al.* Efficient correction of Fabry mice and patient cells mediated by lentiviral transduction of hematopoietic stem/progenitor cells. *Gene Therapy* 2007; **14**: 256 - 265.
20 Hacein-Bey-Abina S, Von Kalle C, Schmidt M, McCormack MP, Wulffraat N, Leboulch P *et al.* LMO2-associated clonal T cell proliferation in two patients after gene therapy for SCID-X1. *Science* 2003; **302**: 415 - 419.
21 Hacein-Bey-Abina S, Garrigue A, Wang GP, Soulier J, Lim A, Morillon E *et al.* Insertional oncogenesis in 4 patients after retrovirus-mediated gene therapy of SCID-X1. *J Clin Invest* 2008; **118**: 3132 - 3142.
22 GlaxoSmithKline. (2010). *Full Prescribing Information Package Insert for Retrovir*.
23 Stone MJ, Sausville EA, Fay JW, Headlee D, Collins RH, Figg WD *et al.* A phase I study of bolus versus continuous infusion of the anti-CD19 immunotoxin, IgG-HD37-dgA, in patients with B-cell lymphoma. *Blood* 1996; **88**: 1188 - 1197.
24 Messmann RA, Vitetta ES, Headlee D, Senderowicz AM, Figg WD, Schindler J *et al.* A phase I study of combination therapy with immunotoxins IgG-HD37-deglycosylated ricin A chain (dgA) and IgG-RFB4-dgA (Combotox) in patients with refractory CD19(+), CD22(+) B cell lymphoma. *Clin Cancer Res* 2000; **6**: 1302 - 1313.
25 Omar RF, Gourde P, Desormeaux A, Tremblay M, Beauchamp D, Bergeron MG. *In vivo* toxicity of foscarnet and zidovudine given alone or in combination. *Toxicol Appl Pharmacol* 1996; **139**: 324 - 332.
26 Tan X, Boudinot FD, Chu CK, Egron D, Perigaud C, Gosselin G *et al.* Pharmacokinetics of bis(t-butyl-SATE)-AZTMP, a bispivaloylthioethyl prodrug for intracellular delivery of zidovudine monophosphate, in mice. *Antivir Chem Chemother* 2000; **11**: 203 - 211.
27 Quevedo MA, Brinon MC. *In vitro* and *in vivo* pharmacokinetic characterization of two novel prodrugs of zidovudine. *Antiviral Res* 2009; **83**: 103 - 111.
28 Wannachaiyasit S, Chanvorachote P, Nimmannit U. A novel anti-HIV dextrin-zidovudine conjugate improving the pharmacokinetics of zidovudine in rats. *AAPS PharmSciTech* 2008; **9**: 840 - 850.
29 Lapalombella R, Zhao X, Triantafillou G, Yu B, Jin Y, Lozanski G *et al.* A novel Raji-Burkitt's lymphoma model for preclinical and mechanistic evaluation of CD52-targeted immunotherapeutic agents. *Clin Cancer Res* 2008; **14**: 569 - 578.

30 Bilello JA, Eiseman JL, Standiford HC, Drusano GL. Impact of dosing schedule upon suppression of a retrovirus in a murine model of AIDS encephalopathy. *Antimicrob Agents Chemother* 1994; **38**: 628 - 631.
31 Kase R, Shimmoto M, Itoh K, Utsumi K, Kotani M, Taya C *et al*. Immunohistochemical characterization of transgenic mice highly expressing human lysosomal alpha-galactosidase. *Biochim Biophys Acta* 1998; **1406**: 260 - 266.
32 Zarate YA, Hopkin RJ. Fabry's disease. *Lancet* 2008; **372**: 1427 - 1435.
33 Amarnath S, Mangus CW, Wang JC, Wei F, He A, Kapoor V *et al*. The PDL1-PD1 Axis Converts Human TH1 Cells into Regulatory T Cells. *Sci Transl Med* 2011; **3**: 111 - 120.
34 Medin JA, Tudor M, Simovitch R, Quirk JM, Jacobson S, Murray GJ *et al*. Correction in trans for Fabry disease: expression, secretion and uptake of alpha-galactosidase A in patient-derived cells driven by a high-titer recombinant retroviral vector. *Proc Natl Acad Sci USA* 1996; **93**: 7917 - 7922.
35 Walia JS, Neschadim A, Lopez-Perez O, Alayoubi A, Fan X, Carpentier S *et al*. Autologous transplantation of lentivector/acid ceramidase-transduced hematopoietic cells in non-human primates. *Hum Gene Ther* 2011; **22**: 679 - 687.
36 Qin G, Takenaka T, Telsch K, Kelley L, Howard T, Levade T *et al*. Preselective gene therapy for Fabry disease. *Proc Natl Acad Sci USA* 2001; **98**: 3428 - 3433.